

## Atom-interferometric study of Bose-Einstein condensation

Thomas P. Altenmüller, Rainer Müller, and Axel Schenzle

*Max-Planck-Institut für Quantenoptik, 85748 Garching, Germany*

*and Sektion Physik der Ludwig-Maximilians-Universität München, Theresienstraße 37, 80333 München, Germany*

(Received 2 January 1997)

We investigate the influence of a Bose-Einstein condensate on the coherence properties of a traversing atomic beam. We derive a master equation describing the interaction between beam atoms and the condensate in *s*-wave approximation. Scattering rates are calculated and compared with the case of an ordinary Boltzmann gas. Special attention is paid to the decoherence of the beam, i.e., the decay of spatial coherence in the presence of the condensate. As an application, we explicitly calculate the visibility of the interference pattern in a double-slit experiment and indicate signs for the onset of the condensation. [S1050-2947(97)02010-6]

PACS number(s): 03.75.Dg

### I. INTRODUCTION

The recent successes in the production of Bose-Einstein condensates in magneto-optical traps [1–4] create a demand for specific means to investigate the condensate. Although commonly used methods like light scattering do produce an image of the condensate's distribution in position or momentum space, these methods are not especially sensitive to the peculiar coherence properties of this "macroscopic quantum state." In particular, there is no clear signature of the onset of the Bose-Einstein condensation. Since coherence is most easily detected in an interferometric experiment, it seems promising to think about an *interferometric* study of Bose-Einstein condensation.

In this article we focus our interest on the possibility of using *atom-interferometric* methods to investigate the condensation process. We consider an atomic probe beam that passes through a diffraction apparatus, i.e., a grating or a beam splitter. Subsequently it traverses a region filled with a gaseous medium. In our case this medium will be either an ordinary Boltzmann gas or a Bose-Einstein condensate. Figure 1 shows the principal setup of such an experiment.

The interaction between the gas and the beam atoms will in general lead to a loss of coherence between spatially separated wave-packet components which manifests itself in a reduced visibility of the diffraction pattern. This is an example of environment-induced decoherence [5]. We study how the interference pattern is altered by the presence of the condensate. This is compared with the case where the beam passes an ordinary Boltzmann gas. The interesting point is that the observation of the visibility may provide a signature for the coherence properties of the gas and especially the onset of condensation.

There are two main advantages in using atomic interferometry instead of light scattering: First, the collisional cross section, roughly estimated by the square of the scattering length, is much smaller than the cross section of near resonant photons which is of the order of the square of the photonic wavelength. Therefore, for the scattering of an atomic beam by a *dilute* gas—as it is realized in the experiments [1–4]—multiple scattering events can be avoided. The information carried by the scattered beam will refer only to a single interaction event. Second, the kinematics of the colli-

sion between a beam of heavy atoms and a gas of light atoms strongly favors forward scattering of the beam whereas, in the case of light scattering, spontaneous emission of a photon from a gas is rather isotropic. Thus using a heavy atomic probe beam one can collect very efficiently information about the condensate with a minimum of scattering events suffered by the gas.

In this article we will consider a condensing *ideal* Bose gas in *free space*. A realistic Bose gas is neither in free space nor ideal but trapped and at least weakly interacting. However, what we want to demonstrate are the qualitative changes in the beam properties due to condensation of the gas.

The organization of the paper is as follows. In Sec. II we derive a master equation in Lindblad form for the interaction between a beam atom and the gas in thermodynamic equilibrium, describing the loss of beam coherence. In the third section we calculate the decoherence rates for a Boltzmann and a Bose gas and compare the two cases. Relating the decoherence rates to the loss of visibility, we discuss the signs for the onset of the condensation. Finally we summarize the results in a conclusion.

### II. MASTER EQUATION FOR AN ATOMIC BEAM IN A GASEOUS ENVIRONMENT

We consider an atomic probe beam in interaction with a gaseous medium. The collisions between gas and beam atoms introduce a dephasing of the beam. We are only interested in the coherence properties of the beam. Therefore we regard the gas as a background medium. It is described as a *reservoir* which can be removed from the beam dynamics by an adiabatic elimination procedure very similar to that in the derivation of quantum optical master equations (i.e., [6,7]). Using a different approach, a master equation for an atom in interaction with a Boltzmann gas has recently been derived in [8]. However, this phenomenologically motivated derivation of a master equation is not valid for a cold gas, which is the situation we would like to describe here. We start from the Hamiltonian of the interaction between beam atoms and gas in second quantization:

$$H = T + T_G + U, \quad (1)$$

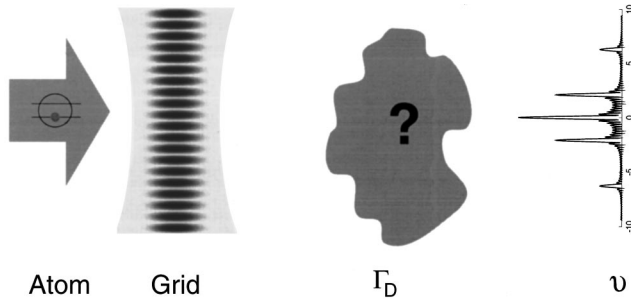


FIG. 1. Principal setup of an atom-interferometric experiment. An incident atomic beam is diffracted at a grid, realized, for example, by a standing light wave. The interference pattern on the screen is characterized by the visibility  $\nu$ . The interaction with a background gas in the path of the atomic beam can be described by the decoherence rate  $\Gamma_D$ .

where  $T$  defines the kinetic energy of the beam atoms,  $T_G$  the kinetic energy of the gas atoms, and  $U$  the interaction potential:

$$\begin{aligned}
 T &= \sum_p \frac{p^2}{2m} \hat{\psi}_p^\dagger \hat{\psi}_p, \\
 T_G &= \sum_{p_G} \frac{p_G^2}{2m_G} \hat{\psi}_{p_G}^\dagger \hat{\psi}_{p_G}, \\
 U &= \sum_{r,r_G} \hat{\psi}_{r_G}^\dagger \hat{\psi}_r^\dagger U(\mathbf{r}-\mathbf{r}_G) \hat{\psi}_r \hat{\psi}_{r_G}. \quad (2)
 \end{aligned}$$

In writing down the Hamiltonian (1), we have assumed an *ideal* background gas. In the Bose-Einstein condensation (BEC) experiments mentioned above, an interaction between the atoms is present, although it is much weaker as in the case of superfluidity. The standard theoretical treatment of the effects of interactions within the Bose condensate makes use of Bogoliubov methods. This scheme is valid at low temperatures ( $T \approx 0$ ). Near the transition temperature  $T_c$ , which is the physical regime we are interested in, it breaks down, however. It is therefore not possible to take the background gas interactions fully into account. An ideal gas treatment is the only viable theoretical approximation to a weakly interacting gas near  $T_c$ , and we will only include the gas-beam interaction in our calculation.

In the following the quantities without index refer to the beam atom while those indexed with  $G$  correspond to the background gas. The two-body potential  $U$  can be decomposed into its Fourier components:

$$U = \sum_q V(\mathbf{q}) \sum_{p,p_G} \hat{\psi}_{p+q}^\dagger \hat{\psi}_{p_G-q}^\dagger \hat{\psi}_p \hat{\psi}_{p_G}. \quad (3)$$

We assume that gas and beam atoms are physically different and can be distinguished. Therefore field operators creating and annihilating gas atoms commute with those for the beam atoms. In an interaction picture with respect to the kinetic energy of the beam and the gas atoms we obtain for the Hamiltonian

$$\begin{aligned}
 H(t) &= \sum_q V(\mathbf{q}) \sum_p \hat{\psi}_{p+q}^\dagger \hat{\psi}_p \\
 &\times e^{(i/\hbar)[(\mathbf{p}+\mathbf{q})^2/2m - p^2/2m]t} \sum_{p_G} \hat{\psi}_{p_G-q}^\dagger \hat{\psi}_{p_G} \\
 &\times e^{(i/\hbar)[(\mathbf{p}_G-\mathbf{q})^2/2m_G - p_G^2/2m_G]t}. \quad (4)
 \end{aligned}$$

For simplicity, we will not mark the operators in the interaction picture. In a perturbative approach, the problem can be solved by considering the equation of motion for the atomic beam's reduced density operator, summing up all orders of ladder diagrams but taking into account only two-body collisions in  $s$ -wave approximation. This is physically justified in the present case of a dilute, low-temperature gas. It is known [11] that it is *formally* equivalent to an approach using second order perturbation theory with factorization of the initial conditions and the replacement of the coupling constants by an expression involving the actual scattering cross section as obtained in all orders of perturbation theory.

#### A. Iteration of the von Neumann equation

Pursuing the above line of reasoning, we formally iterate the von Neumann equation for the interaction Hamiltonian in Eq. (4),

$$\dot{\rho}_{A+G} = \frac{1}{i\hbar} [H(t), \rho_{A+G}], \quad (5)$$

and obtain

$$\begin{aligned}
 \dot{\rho}_{A+G}(t) &= \frac{1}{i\hbar} [H(0), \rho_{A+G}(0)] \\
 &- \frac{1}{\hbar^2} \int_0^t d\tau [H(t), [H(t-\tau), \rho_{A+G}(t-\tau)]]. \quad (6)
 \end{aligned}$$

Before the beam reaches the gas the total density operator factorizes into the beam's initial state  $\rho(0)$  and the initial state of the gas,  $\rho_G(0)$ . Virtually no beam atom will encounter the same gas atom twice before the gas rethermalizes. Therefore the reservoir of background atoms remains in its stationary state for all time. We assume that a factorization is practically valid at any time before gas and atom interact:

$$\rho_{A+G}(t-\tau) = \rho(t-\tau) \otimes \rho_G(0). \quad (7)$$

Assuming thermal equilibrium, we trace over the gas degrees of freedom and obtain an equation of motion for the beam atoms alone. We neglect many-body effects in the atomic beam. This allows us a single-atom description of the beam, and we use a bra-ket notation for the beam operators. After some rearrangement we find

$$\begin{aligned}
\dot{\rho}(t) &= -\frac{1}{\hbar^2} \int_0^t d\tau \text{Tr}_G \{ [\tilde{H}(t), [\tilde{H}(t-\tau), \rho(t-\tau) \otimes \rho_G(0)]] \} \\
&= -\frac{1}{\hbar^2} \int_0^t d\tau \sum_{p_G, q, q'} \tilde{n}(\mathbf{p}_G) |V(\mathbf{q})|^2 \left\{ \sum_p e^{i/\hbar \tau (E_i - E_f)} |\mathbf{p}\rangle \right. \\
&\quad \times \langle \mathbf{p} | \rho(t-\tau) - \sum_{p, p'} e^{i/\hbar \tau (E'_i - E'_f)} | \mathbf{p}' + \mathbf{q} \rangle \\
&\quad \left. \times \langle \mathbf{p}' | (t) \rho(t-\tau) | \mathbf{p} \rangle \langle \mathbf{p} + \mathbf{q} | (t) \right\} + \text{H.c.} \quad (8)
\end{aligned}$$

Here, the kinetic energy of the system consisting of beam and gas is  $E_i$  before and  $E_f$  after the collision:

$$E_i = \frac{p^2}{2m} + \frac{p_G^2}{2m_G}, \quad (9)$$

$$E_f = \frac{(\mathbf{p} + \mathbf{q})^2}{2m} + \frac{(\mathbf{p}_G - \mathbf{q})^2}{2m_G}. \quad (10)$$

The energies  $E'_i$  and  $E'_f$  refer to the momentum  $\mathbf{p}'$ . The quantity  $\tilde{n}(\mathbf{p}_G)$  in Eq. (8) denotes the ‘‘effective population’’ of the gas one-particle momentum state  $|\mathbf{p}_G\rangle$  in thermal equilibrium. It is defined as the expectation value of the gas operators in the doubly iterated interaction Hamiltonian:

$$\tilde{n}(\mathbf{p}_G) \delta_{p_G, p_{G'}} = \text{Tr}_G \{ \hat{\psi}_{p_G}^\dagger \hat{\psi}_{p_G - q'} \hat{\psi}_{p_G - q} \hat{\psi}_{p_G} \rho_G(0) \}. \quad (11)$$

### B. Effective population $\tilde{n}(\mathbf{p}_G)$

All thermal properties of the gas reservoir are represented by the effective population  $\tilde{n}(\mathbf{p}_G)$  of the state  $|\mathbf{p}_G\rangle$ . In the case of an ideal Boltzmann gas  $\rho_G(0)$  is given by

$$\rho_G = \frac{N}{Z} e^{-\beta p_G^2 / 2m_G}, \quad (12)$$

where  $\beta = 1/kT$  defines as usual the inverse temperature,  $N$  is the total number of gas atoms, and  $Z$  the partition function. Since the field creation and annihilation operators  $\hat{\psi}_{p_G}^\dagger$  and  $\hat{\psi}_{p_G}$  for a classical Boltzmann gas commute,  $\tilde{n}(\mathbf{p}_G)$  is readily evaluated:

$$\tilde{n}(\mathbf{p}_G) = \delta_{q, q'} n_B(\mathbf{p}_G) = \delta_{q, q'} \frac{N}{Z} e^{-\beta p_G^2 / 2m_G}. \quad (13)$$

For a Bose gas we have to take care of the bosonic commutation relation for the field operators:

$$[\hat{\psi}_k, \hat{\psi}_{k'}^\dagger] = \delta_{kk'}. \quad (14)$$

Applying Eq. (14) to Eq. (11) we obtain for the effective population number  $\tilde{n}(\mathbf{p}_G)$ ,

$$\begin{aligned}
\tilde{n}(\mathbf{p}_G) \delta_{p_G, p_{G'}} &= \text{Tr}_G \{ \hat{\psi}_{p_G}^\dagger \hat{\psi}_{p_G} \delta_{p_G - q', p_G - q} \rho_G(0) \} \\
&\quad + \text{Tr}_G \{ \hat{\psi}_{p_G}^\dagger \hat{\psi}_{p_G - q} \hat{\psi}_{p_G - q'} \hat{\psi}_{p_G} \rho_G(0) \}. \quad (15)
\end{aligned}$$

Since the thermal equilibrium density operator of the gas is diagonal in the momentum representation, the first term on the right hand side of Eq. (15) simply results in the population number  $n_{\text{BE}}(\mathbf{p}_G)$  of the momentum state  $|\mathbf{p}_G\rangle$  as given by the one-particle density operator:

$$\begin{aligned}
&\text{Tr}_G \{ \hat{\psi}_{p_G}^\dagger \hat{\psi}_{p_G} \delta_{p_G - q', p_G - q} \rho_G(0) \} \\
&= \delta_{qq'} \text{Tr}_G \{ \hat{\psi}_{p_G}^\dagger \hat{\psi}_{p_G} \rho_G(0) \} = n_{\text{BE}}(\mathbf{p}_G) \delta_{qq'} \delta_{p_G, p_{G'}}. \quad (16)
\end{aligned}$$

Here,  $n_{\text{BE}}(\mathbf{p}_G)$  is the population number according to Bose-Einstein statistics:

$$n_{\text{BE}}(\mathbf{p}_G) = \frac{1}{\exp\{\beta(p_G^2/2m_G - \mu)\} - 1}, \quad (17)$$

where  $\mu < 0$  is the chemical potential for the Bose gas. The second right hand side term of Eq. (15) describes the creation and annihilation of two particles (in normal ordering). For  $q, q' \neq 0$  [otherwise the integrand of the  $q$ -space integration in Eq. (8) vanishes anyway] we obtain

$$\begin{aligned}
&\text{Tr}_G \{ \hat{\psi}_{p_G}^\dagger \hat{\psi}_{p_G - q} \hat{\psi}_{p_G - q'} \hat{\psi}_{p_G} \rho_G(0) \} \\
&= \text{Tr}_G \{ \hat{\psi}_{p_G}^\dagger \hat{\psi}_{p_G} \hat{\psi}_{p_G - q} \hat{\psi}_{p_G - q'} \rho_G(0) \} \\
&= \delta_{p_G, p_{G'}} \delta_{qq'} \text{Tr}_G \{ \hat{n}_{p_G} \hat{n}_{p_G - q} \rho_G(0) \} \\
&= \delta_{p_G, p_{G'}} \delta_{qq'} n_{\text{BE}}(\mathbf{p}_G) n_{\text{BE}}(\mathbf{p}_G - \mathbf{q}). \quad (18)
\end{aligned}$$

Collecting these results yields the effective population of state  $|\mathbf{p}_G\rangle$  for a bosonic gas:

$$\tilde{n}(\mathbf{p}_G) = \delta_{qq'} n_{\text{BE}}(\mathbf{p}_G) [1 + n_{\text{BE}}(\mathbf{p}_G - \mathbf{q})]. \quad (19)$$

Compared with a Boltzmann gas the effective population of the gas momentum state  $|\mathbf{p}_G\rangle$  in a Bose gas is altered due to a typical bosonic enhancement factor of  $[1 + n_{\text{BE}}(\mathbf{p}_G - \mathbf{q})]$ .

How does the effective population defined in Eq. (19) change with temperature? At very low temperatures,  $n_{\text{BE}}(\mathbf{p}_G)$  is very small except for  $\mathbf{p}_G = \mathbf{0}$ . Since the additional bosonic contribution involves the product  $n_{\text{BE}}(\mathbf{p}_G) n_{\text{BE}}(\mathbf{p}_G - \mathbf{q})$ , i.e., the bosonic population number at two different momenta, the bosonic enhancement will vanish at  $T=0$ , because only one of the two factors can be nonzero at  $T=0$ . At temperatures much higher than the critical temperatures  $T_c$ , on the other hand, the distribution  $n_{\text{BE}}(\mathbf{p}_G)$  becomes classical for BEC in a gas with a fixed number of particles: For an ideal free particle gas the fugacity  $e^{\beta\mu}$  behaves at  $T \gg T_c$  asymptotically as [9]

$$e^{\beta\mu} \sim \left( \frac{T_c}{T} \right)^{3/2} \zeta \left( \frac{3}{2} \right) \ll 1, \quad T \gg T_c. \quad (20)$$

Therefore, in the high-temperature limit,  $n_{\text{BE}}(\mathbf{p}_G)$  can be expanded as

$$n_{\text{BE}}(\mathbf{p}_G) \sim e^{\beta\mu} e^{-\beta p_G^2/2m_G} \ll 1, \quad T \gg T_c \quad \text{for all } \mathbf{p}_G. \quad (21)$$

The additional contribution to the scattering in a Bose gas will therefore be negligible for  $T \gg T_c$ . Only in an intermediate regime of  $T \approx T_c$  is the bosonic enhancement non-negligible. For  $T \approx T_c$ , a considerable departure from the behavior of a Boltzmann gas can be expected.

### C. *s*-wave scattering

Taking advantage of the thermal blurring of the position of the gas atoms on the length scale of the gas's thermal de Broglie wavelength  $\lambda_{\text{dB}}$ ,

$$\lambda_{\text{dB}} = \hbar \sqrt{\frac{\beta}{2m_G}}, \quad (22)$$

we will approximate the interaction potential  $U(\mathbf{r}-\mathbf{r}_G)$  by a hard-core  $\delta$  potential, since distances smaller than  $\lambda_{\text{dB}}$  are not resolved:

$$U(\Delta\mathbf{r}) = U_0 \delta(\Delta\mathbf{r}). \quad (23)$$

This, of course, implies a flat pseudopotential  $V(\mathbf{q})$ . In *s*-wave scattering at a hard-core  $\delta$  potential the pseudopotential  $V(\mathbf{q}) = V(0) = U_0/V$  is connected to the scattering amplitude  $f$  by [10]

$$f = -\frac{1}{4\pi} \int d^3\mathbf{r} e^{-i\mathbf{k}\cdot\mathbf{r}} \frac{2m_{\text{red}}}{\hbar^2} U(\mathbf{r}) = -\frac{1}{4\pi} \frac{2m_{\text{red}}}{\hbar^2} U_0. \quad (24)$$

For the scattering of two distinguishable particles, namely, the gas atom and the beam atom, the scattering amplitude  $f$ , respectively, the scattering length  $a = -f$ , is related to the total cross section by

$$\sigma = \int d\Omega |f(\Omega)|^2 = 4\pi |f|^2 = 4\pi a^2. \quad (25)$$

Therefore with the help of Eqs. (25) and (24) we will replace the Fourier transform of the potential  $V(\mathbf{q})$  by an expression involving the total scattering cross section  $\sigma$ :

$$|V(\mathbf{q})|^2 = \frac{1}{V^2} \frac{\sigma \pi \hbar^4}{m_{\text{red}}^2}. \quad (26)$$

Note that  $\sigma$  represents the actual total cross section, as found by considering all orders of the Born series. This enables us to treat consistently singular hard-core potentials as in Eq. (23) (cf. [11]).

### D. Master equation and scattering rates

The iterated von Neumann equation (8) is an integro-differential equation and is therefore delocalized in time: An exact solution requires the knowledge of  $\rho(t)$  for all times  $t$ . In order to obtain from Eq. (8) a master equation local in time we will perform in Eq. (8) the Born-Markov approxi-

mation which effectively consists in neglecting the  $\tau$  dependence of the beam's density operator and in shifting the upper limit of the  $\tau$  integration to infinity.

This approximation is valid in the present case since it can be shown by averaging Eq. (8) over all possible momentum transfers that the time scale for the decay of correlations is  $\hbar/E_{\text{c.m.}}$  (where  $E_{\text{c.m.}}$  is the kinetic energy in the center-of-mass system). Thus, even for a cold gas (Boltzmann or Bose-Einstein), the correlations between gas and beam decay fast, provided the kinetic energy of the collision in the center-of-mass system is large enough. This is analogous to the situation considered in the quantum optical master equation where the correlation time is essentially set by the inverse transition frequency [7].

After the Born-Markov approximation, the master equation has the form

$$\begin{aligned} \dot{\rho}(t) = & - \sum_{q,p} \frac{1}{2} \Gamma(\mathbf{p}, \mathbf{q}) \{ |\mathbf{p}\rangle \langle \mathbf{p}| \rho(t) + \rho(t) |\mathbf{p}\rangle \langle \mathbf{p}| \} \\ & + \sum_{q,p,p'} \frac{1}{2} \{ \Gamma(\mathbf{p}, \mathbf{q}) + \Gamma(\mathbf{p}', \mathbf{q}) \} |\mathbf{p}' + \mathbf{q}\rangle \\ & \times \langle \mathbf{p}' | (t) \rho(t) | \mathbf{p}\rangle \langle \mathbf{p} + \mathbf{q} | (t). \end{aligned} \quad (27)$$

Here, we have defined scattering rates  $\Gamma(\mathbf{p}, \mathbf{q})$ :

$$\Gamma(\mathbf{p}, \mathbf{q}) = \frac{1}{\hbar} \sum_{p_G} \tilde{n}(\mathbf{p}_G) |V(\mathbf{q})|^2 2\pi \delta(E_i - E_f), \quad (28)$$

which contains the integration over all possible gas momenta  $\mathbf{p}_G$ .

Using the explicit form (26) for  $|V(\mathbf{q})|^2$ , the scattering rate for the Boltzmann gas becomes

$$\begin{aligned} \Gamma(\mathbf{p}, \mathbf{q}) = & n \sigma \bar{v}_B \frac{1}{2\pi} \left[ \frac{\lambda_{\text{dB}} q (1 + \delta)}{2\hbar} \right]^2 \frac{(2\pi\hbar)^3}{q^3 V} \\ & \times \exp \left\{ - \left( \frac{\lambda_{\text{dB}}}{2\hbar} \right)^2 (1 + \delta)^2 \left( q + \frac{2\delta}{1 + \delta} p \cos\theta \right)^2 \right\}, \end{aligned} \quad (29)$$

where  $n$  is the gas density,

$$\delta = \frac{m_G}{m} \quad (30)$$

is the mass ratio, and  $\bar{v}_B$  the average velocity of atoms in a Boltzmann gas,

$$\bar{v}_B = \frac{2\hbar}{\sqrt{\pi m_G \lambda_{\text{dB}}}}. \quad (31)$$

Note that the contributions to  $\Gamma(\mathbf{p}, \mathbf{q})$  decay with increasing  $\mathbf{q}$  according to a Gaussian profile in  $\mathbf{q}$ . Thus all details of the interatomic potential on a length scale smaller than  $\lambda_{\text{dB}}$  are damped out and irrelevant. This is consistent with the *s*-wave approximation used here (cf. Sec. II C).

Similarly, the scattering rate for the Bose gas is defined by

$$\Gamma(\mathbf{p}, \mathbf{q}) = \frac{2\pi}{\hbar} |V(\mathbf{q})|^2 \sum_{\mathbf{p}_G} n_{\text{BE}}(\mathbf{p}_G) [1 + n_{\text{BE}}(\mathbf{p}_G - \mathbf{q})] \times \delta(E_i - E_f). \quad (32)$$

Transforming the discrete sum over  $\mathbf{p}_G$  in a continuous integral we must consider the gas phase with a condensate separately, which arises below the critical point because the continuous phase space cannot accommodate all gas atoms. The transformation is

$$\begin{aligned} & \sum_{\mathbf{p}_G} n_{\text{BE}}(\mathbf{p}_G) [1 + n_{\text{BE}}(\mathbf{p}_G - \mathbf{q})] \\ & \rightarrow \frac{V}{(2\pi\hbar)^3} \int d^3\mathbf{p}_G \left( N_0 \frac{(2\pi\hbar)^3}{V} \delta(\mathbf{p}_G) + n_{\text{BE}}(\mathbf{p}_G) \right) \\ & \times \left[ 1 + \left( N_0 \frac{(2\pi\hbar)^3}{V} \delta(\mathbf{p}_G - \mathbf{q}) + n_{\text{BE}}(\mathbf{p}_G - \mathbf{q}) \right) \right], \quad (33) \end{aligned}$$

where  $N_0$  is the number of atoms in the free space condensate,

$$N_0 = N \left[ 1 - \left( \frac{T}{T_c} \right)^{3/2} \right] [1 - \theta(T - T_c)], \quad (34)$$

and  $T_c$  is the critical temperature for a fixed number of gas atoms in a constant volume:

$$T_c = \left( \frac{N}{V \zeta(3/2)} \right)^{2/3} \frac{2\pi\hbar^2}{m_G k}. \quad (35)$$

The coexistence of two phases motivates the separation of the total scattering rate  $\Gamma(\mathbf{p}, \mathbf{q})$  into a rate  $\Gamma^\epsilon(\mathbf{p}, \mathbf{q})$  for scattering by the excited phase (including the bosonic enhancement due to events which scatter a gas atom into the condensate), and a rate  $\Gamma^0(\mathbf{p}, \mathbf{q})$  for scattering by the condensate.

$$\Gamma(\mathbf{p}, \mathbf{q}) = \Gamma^\epsilon(\mathbf{p}, \mathbf{q}) + \Gamma^0(\mathbf{p}, \mathbf{q}). \quad (36)$$

Using the transformation (33) we obtain for the rate of scattering by the excited phase after some manipulations

$$\begin{aligned} \Gamma^\epsilon(\mathbf{p}, \mathbf{q}) &= \frac{2\pi}{\hbar} |V(\mathbf{q})|^2 \frac{V}{(2\pi\hbar)^3} \int d^3\mathbf{p}_G n_{\text{BE}}(\mathbf{p}_G) [1 + n_{\text{BE}}(\mathbf{p}_G)] \delta(E_i - E_f) + \frac{2\pi}{\hbar} |V(\mathbf{q})|^2 n_{\text{BE}}(-\mathbf{q}) N_0 \delta\left(\mathbf{p} \cdot \mathbf{q} \left( \frac{1}{m_G} - \frac{1}{m} \right) - \frac{q^2}{2\mu}\right) \\ &= \frac{(2\pi\hbar)^3}{q^3 V} n_{\epsilon} \sigma \bar{v}_{\text{BE}} \frac{1}{2\pi g_2(z)} \left[ \frac{\lambda_{\text{dB}} q (1 + \delta)}{2\hbar} \right]^2 \frac{1}{1 - e^{\lambda_{\text{dB}}^2 \delta / \hbar^2 (q^2 + 2pq \cos \theta)}} \\ & \times \ln \left[ \frac{1 - z \exp\left\{ -\frac{1}{4} \left( \frac{\lambda_{\text{dB}}}{\hbar} \right)^2 (1 + \delta)^2 \left( q + \frac{2\delta}{1 + \delta} p \cos \theta \right)^2 \right\}}{1 - z \exp\left\{ -\frac{1}{4} \left( \frac{\lambda_{\text{dB}}}{\hbar} \right)^2 (1 + \delta)^2 \left( q + \frac{2\delta}{1 + \delta} p \cos \theta \right)^2 + \left( \frac{\lambda_{\text{dB}}}{\hbar} \right)^2 (q^2 + 2pq \cos \theta) \delta \right\}} \right] \\ & + \frac{(2\pi\hbar)^3}{V} n_0 \sigma n_{\text{BE}}(-\mathbf{q}) \frac{1}{4\pi} \frac{(1 + \delta)^2}{m_G^2} \delta\left(\mathbf{p} \cdot \mathbf{q} \left( \frac{1}{m_G} - \frac{1}{m} \right) - \frac{q^2}{2\mu}\right), \quad (37) \end{aligned}$$

where  $n_0 = N_0/V$  designates the condensate density and  $\bar{v}_{\text{BE}}$  the average velocity of an atom in a Bose gas,

$$\bar{v}_{\text{BE}} = \frac{2\hbar}{\sqrt{\pi m_G \lambda_{\text{dB}}}} \frac{g_2(z)}{g_{3/2}(z)}. \quad (38)$$

Here  $z$  is the fugacity,

$$z = e^{\beta\mu}, \quad (39)$$

and the functions  $g_j(z)$  are defined as usual by

$$g_j(z) = \frac{1}{\Gamma(j)} \int_0^\infty dx \frac{x^{j-1}}{e^{x/z} - 1}. \quad (40)$$

The scattering rate by the condensate is:

$$\begin{aligned} \Gamma^0(\mathbf{p}, \mathbf{q}) &= \frac{(2\pi\hbar)^3}{V} n_0 \sigma \frac{1}{4\pi} \frac{(1 + \delta)^2}{m_G^2} [1 + n_{\text{BE}}(-\mathbf{q})] \\ & \times \delta\left(\frac{\mathbf{p} \cdot \mathbf{q}}{m} + \frac{q^2}{2\mu}\right). \quad (41) \end{aligned}$$

The scattering rate  $\Gamma(\mathbf{p}, \mathbf{q})$  describes the dependence of the momentum transfer  $\mathbf{q}$  on the beam momentum  $\mathbf{p}$ . Energy and momentum conservation are included in the scattering rates, thus selecting the possible values of the momentum transfer  $\mathbf{q}$  for a given  $\mathbf{p}$  and a fixed distribution of the gas momenta  $\mathbf{p}_G$ . The ‘‘resonance condition’’ for zero gas momentum,

$$\frac{\mathbf{p} \cdot \mathbf{q}}{m} + \frac{q^2}{2\mu} = 0, \quad (42)$$

is exactly fulfilled for scattering by the condensate [cf. Eq. (41)].

### E. Lindblad form of the master equation

So far we have derived a Hermitian master equation with constant trace for the dynamics of a beam atom that scatters off a Boltzmann or Bose gas in thermal equilibrium. Treating the problem, we concentrate on two-body collisions and *s*-wave scattering. Although the dynamics of the beam's momentum *distribution* due to collisions with the gas is well described by Eq. (27), a correct treatment of the coherence properties demands the positivity of the density operator. This requirement is fulfilled if the master equation can be brought into Lindblad form:

$$\dot{\rho} = - \sum_i \left\{ \frac{1}{2} F_i^\dagger F_i \rho + \frac{1}{2} \rho F_i^\dagger F_i - F_i \rho F_i^\dagger \right\}. \quad (43)$$

However, it is not possible to cast Eq. (27) exactly into the Lindblad form (43). This problem occurs generally in situations where a continuous energy spectrum of the operators produces a continuous range of oscillation frequencies in the interaction picture: Because the evaluation of the  $\delta$  functions, which leads to Eq. (27) being performed once from the left and once from the right side of  $\rho$ , the resonant oscillation frequencies in Eq. (27) corresponding to these two possibilities in general are not equal, thus rendering the statistical weights different, albeit the corresponding combinations of operators are the same. Since the oscillation frequencies are arbitrarily close to each other, these cross terms cannot be removed by a secular approximation as, for example, in the master equation for a multilevel atom with well separated discrete energy levels.

Nevertheless, if the variance of the beam velocity  $\Delta v = \Delta p/m$  is small compared with the width of the thermal velocity distribution of the gas [ $\approx \hbar/(\lambda_{dB}m)$ ] so that the condition

$$1 \gg \delta \lambda_{dB} \Delta p / \hbar \quad (44)$$

is fulfilled, i.e., if the beam is monochromatic compared with its gas environment, we can approximate

$$\frac{1}{2} [\Gamma(\mathbf{p}, \mathbf{q}) + \Gamma(\mathbf{p}', \mathbf{q})] \approx \sqrt{\Gamma(\mathbf{p}, \mathbf{q})} \sqrt{\Gamma(\mathbf{p}', \mathbf{q})}. \quad (45)$$

This factorization of the scattering rates replaces the arithmetic mean by the geometric mean. Using this approximation we obtain from Eq. (27) the master equation

$$\begin{aligned} \dot{\rho} = & - \sum_q \left\{ \frac{1}{2} \sum_p \Gamma(\mathbf{p}, \mathbf{q}) |\mathbf{p}\rangle \langle \mathbf{p}| \rho + \frac{1}{2} \rho \sum_p \Gamma(\mathbf{p}, \mathbf{q}) |\mathbf{p}\rangle \langle \mathbf{p}| \right. \\ & - \left( \sum_{p'} \sqrt{\Gamma(\mathbf{p}', \mathbf{q})} |\mathbf{p}' + \mathbf{q}\rangle \langle \mathbf{p}'| \right) \\ & \left. \times \rho \left( \sum_p \sqrt{\Gamma(\mathbf{p}, \mathbf{q})} |\mathbf{p}\rangle \langle \mathbf{p} + \mathbf{q}| \right) \right\}, \quad (46) \end{aligned}$$

which is equivalent to the Lindblad form in Eq. (43) with

$$F_q = \sum_p \sqrt{\Gamma(\mathbf{p}, \mathbf{q})} |\mathbf{p} + \mathbf{q}\rangle \langle \mathbf{p}|. \quad (47)$$

However, at very low temperatures, as, for example, when the condensate forms, condition (44) is not well obeyed. In this case we take advantage of the special setup studied here: For an atomic *beam* we assume

$$p \gg \Delta p. \quad (48)$$

Since we deal with heavy beam atoms ( $\delta \ll 1$ ) even for slightly different  $\mathbf{p}$  and  $\mathbf{p}'$  the same momentum transfers  $\mathbf{q}$  are selected by the scattering rates so that we can substitute

$$\frac{1}{2} [\Gamma(\mathbf{p}, \mathbf{q}) + \Gamma(\mathbf{p}', \mathbf{q})] \approx \Gamma(\bar{\mathbf{p}}, \mathbf{q}), \quad (49)$$

using an average beam momentum  $\bar{\mathbf{p}}$  instead of  $\mathbf{p}$  and  $\mathbf{p}'$ . This results in a simple master equation in Lindblad form describing the scattering of an atomic beam at a low-temperature condensate:

$$\dot{\rho}(t) = - \sum_q \Gamma(\bar{\mathbf{p}}, \mathbf{q}) [\rho(t) - e^{(i/\hbar)\mathbf{q} \cdot \hat{\mathbf{r}}(t)} \rho(t) e^{-(i/\hbar)\mathbf{q} \cdot \hat{\mathbf{r}}(t)}]. \quad (50)$$

This equation will allow us to study the loss of beam coherence due to the collisions with a background gas and the consequences for the visibility of the interference pattern.

Let us comment briefly on the status of the approximations required in the derivation of the master equation. The main assumption is that the background gas acts as a reservoir with a fast decay of correlations. The Lindblad form is then necessary for the positivity of the density matrix. A consistent calculational scheme is therefore only possible if the physical conditions allow us to perform the further approximations required for the Lindblad form. In the present section, this has been shown for two cases: for a beam which is monochromatic compared with the gas environment, and for a beam with a very low momentum spread ( $\Delta p \ll p$ ). The last condition is met in a typical atom optics experiment.

### III. DECOHERENCE AND VISIBILITY

In order to apply the master equations (46) and (50) to the problem of an atomic beam traversing a diffraction apparatus and a background gas before being detected on a screen we transform the master equations back from the interaction picture. In the position representation we obtain from Eq. (46) the equation of motion for the beam coherence between points  $\mathbf{r}$  and  $\mathbf{r}'$ :

$$\begin{aligned}
\dot{\rho}(\mathbf{r}, \mathbf{r}') &= \frac{1}{i\hbar} \left[ \frac{\hat{p}^2}{2m}, \rho \right]_{\mathbf{r}, \mathbf{r}'} - \sum_{\mathbf{q}, \mathbf{p}, \mathbf{r}''} \frac{1}{2} \Gamma(\mathbf{p}, \mathbf{q}) \\
&\times \{ e^{(i/\hbar)\mathbf{p} \cdot (\mathbf{r} - \mathbf{r}'')} \rho(\mathbf{r}'', \mathbf{r}') + \rho(\mathbf{r}, \mathbf{r}'') e^{(i/\hbar)\mathbf{p} \cdot (\mathbf{r}'' - \mathbf{r}')} \} \\
&+ \sum_{\mathbf{q}} e^{i/\hbar \mathbf{q} \cdot (\mathbf{r} - \mathbf{r}')} \left( \sum_{\mathbf{p}', \mathbf{r}''} \sqrt{\Gamma(\mathbf{p}', \mathbf{q})} e^{i/\hbar \mathbf{p}' \cdot (\mathbf{r} - \mathbf{r}'')} \right) \\
&\times \rho(\mathbf{r}'', \mathbf{r}''') \left( \sum_{\mathbf{p}, \mathbf{r}'''} \sqrt{\Gamma(\mathbf{p}, \mathbf{q})} e^{i/\hbar \mathbf{p} \cdot (\mathbf{r}''' - \mathbf{r}')} \right). \quad (51)
\end{aligned}$$

From Eq. (51) we see that in principle the decay of coherence between two positions  $\mathbf{r}$  and  $\mathbf{r}'$  involves a nonlocal average in position space. However, the radius of the average depends reciprocally on the width of the scattering rate  $\Gamma(\mathbf{p}, \mathbf{q})$  in momentum space which we assumed to be large [cf. Eq. (44)]. Hence we consistently perform one further approximation in Eq. (51) by replacing the scattering rate by its average:

$$\begin{aligned}
\sum_{\mathbf{p}} \sqrt{\Gamma(\mathbf{p}, \mathbf{q})} e^{(i/\hbar)\mathbf{p} \cdot (\mathbf{r} - \mathbf{r}'')} &\simeq \sqrt{\Gamma(\bar{\mathbf{p}}, \mathbf{q})} \sum_{\mathbf{p}} e^{(i/\hbar)\mathbf{p} \cdot (\mathbf{r} - \mathbf{r}'')} \\
&= \sqrt{\Gamma(\bar{\mathbf{p}}, \mathbf{q})} V \delta(\mathbf{r} - \mathbf{r}''). \quad (52)
\end{aligned}$$

Substituting this into Eq. (51) we obtain

$$\dot{\rho}(\mathbf{r}, \mathbf{r}') = \frac{1}{i\hbar} \left[ \frac{\hat{p}^2}{2m}, \rho \right]_{\mathbf{r}, \mathbf{r}'} - \Gamma_D(|\mathbf{r} - \mathbf{r}'|) \rho(\mathbf{r}, \mathbf{r}'), \quad (53)$$

where  $\Gamma_D(|\mathbf{r} - \mathbf{r}'|)$  defines the decoherence rate between wave-packet components at the positions  $\mathbf{r}$  and  $\mathbf{r}'$ :

$$\Gamma_D(|\mathbf{r} - \mathbf{r}'|) = \sum_{\mathbf{q}} (1 - e^{(i/\hbar)\mathbf{q} \cdot (\mathbf{r} - \mathbf{r}')}) \Gamma(\bar{\mathbf{p}}, \mathbf{q}). \quad (54)$$

The structure of this formula is as follows: The decoherence rate is obtained by summing up all possible variations in the beam atom's phase due to the randomly directed recoil in the collision with the background gas. The momentum transfers  $\mathbf{q}$  will be selected according to the scattering rate  $\Gamma(\mathbf{p}, \mathbf{q})$ . Note that the loss of coherence only depends on the distance  $\Delta = |\mathbf{r} - \mathbf{r}'|$  between the components of the beam.

Equation (53) is of course the same result we would have obtained if we had re-transformed Eq. (50) from the kinetic frame to the position representation. Therefore the following results are equally valid for a beam traversing a Bose gas or a Boltzmann gas. In the following we will focus on the loss of transverse coherence. This is realistic when we consider as diffraction apparatus a grating or double slit.

#### A. Decoherence in a Boltzmann gas

Setting  $\Delta x_{\parallel} = 0$ , we obtain for the transverse decoherence rate of the atomic beam due to collisions with a Boltzmann gas

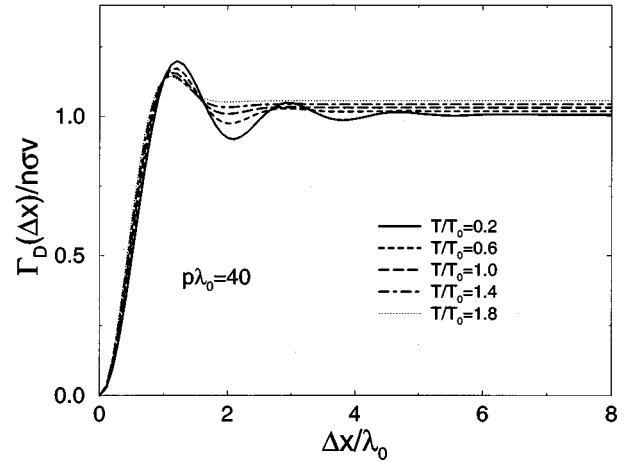


FIG. 2. The decoherence rate  $\Gamma_D(\Delta x)$  due to collisions of a fast atomic beam in a Boltzmann gas versus the width of the coherence  $\Delta x$ . The parameters are  $p\lambda_0/\hbar = 40$  and  $\delta = 0.1$  ( $\lambda_0$  is the gas's thermal de Broglie wavelength at a temperature  $T_0$ ).  $\Gamma_D$  is given in units of the collision rate of the beam at a resting gas,  $n\sigma v = n\sigma p/m$ ,  $\Delta x$  in units of the thermal de Broglie wavelength of the gas at a reference temperature  $T_0$ . Since the beam is fast the decoherence strength is essentially given by the beam's collision rate at a resting gas. An increase in the gas temperature leads to a further, but small increase in the collision rate. The typical length scale of the decoherence is hardly temperature dependent, but given by the de Broglie wavelength of the momentum transfer,  $\hbar/q \approx \hbar/p(1 + \delta)/\delta$ . Because this is rather sharply defined there are oscillations in  $\Gamma_D(\Delta x)$ , which will wash out with increasing temperature.

$$\begin{aligned}
\Gamma_D(\Delta x_{\perp}) &= n\sigma \bar{v} \int d\cos\theta \int dk k e^{-(k+w)^2} \\
&\times \left[ 1 - J_0 \left( k \sin\theta \frac{2}{1 + \delta} \frac{\Delta x_{\perp}}{\lambda_{\text{dB}}} \right) \right], \quad (55)
\end{aligned}$$

where we use the abbreviations

$$k = \frac{\lambda_{\text{dB}} q}{2\hbar} (1 + \delta), \quad w = \frac{1}{\hbar} |\bar{\mathbf{p}}| \lambda_{\text{dB}} \delta \cos\theta. \quad (56)$$

Figures 2 and 3 show the (numerically evaluated) decoherence rates according to Eq. (55). Figure 2 treats the situation of an atomic beam that is fast compared with the thermal velocities of the gas. The relevant length scale  $\lambda_D$  for the decoherence is set by the de Broglie wavelength of the beam, scaled by a mass factor,

$$\lambda_D = \frac{\delta + 1}{\delta} \frac{\hbar}{p}. \quad (57)$$

The strength of decoherence is governed by the rate of collisions  $\Gamma_c$  between gas and beam [cf. Eq. (54)],

$$\Gamma_c = \sum_{\mathbf{q}} \Gamma(\mathbf{p}, \mathbf{q}). \quad (58)$$

For a fast beam,  $\Gamma_c$  is basically given by the collision rate of the beam with resting gas atoms, i.e.,  $\Gamma_c \approx n\sigma v$ , where  $v$  is the beam velocity. In this case, the decoherence rate reflects

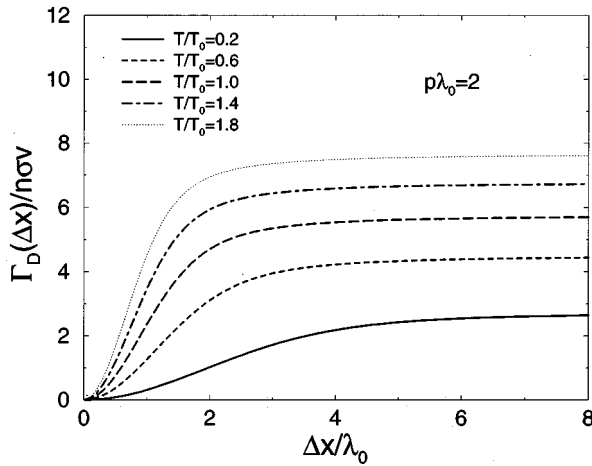


FIG. 3. The decoherence rate  $\Gamma_D(\Delta x)$  due to collisions of a slow atomic beam in a Boltzmann gas. The parameters are  $\rho\lambda_0/\hbar=2$  and  $\delta=0.1$ .  $\Gamma_D$  is given in units of the collision rate at a resting gas,  $\Delta x$  in units of the thermal de Broglie wavelength in the gas at temperature  $T_0$ . The decoherence length is given by the de Broglie wavelength of the gas, the decoherence strength is given by the collision rate. Since the gas velocities decrease with decreasing temperature the collision rate and thus the decoherence strength are decreasing.

basically the properties of the beam itself. However, the background gas subtly leaves its trace in the damping of the oscillations in the decoherence rate with increasing gas temperature.

In Fig. 3 the opposite situation of a slow atomic beam is shown. Here, the length scale of decoherence is given by the thermal de Broglie wavelength of the gas, and the strength of the decoherence is set by the rate of collisions between the thermally moving gas atoms and the beam atoms. Thus with decreasing temperature the decoherence gets weaker because of the increasing thermal de Broglie wavelength and the decreasing rate of collisions.

### B. Decoherence in a Bose gas

For a Bose background gas the decoherence rate can be split up in a contribution due to the scattering at the excited

phase and, if present, a contribution due to collisions with the condensate:

$$\Gamma_D(|\mathbf{r}-\mathbf{r}'|)=\Gamma_D^\epsilon(|\mathbf{r}-\mathbf{r}'|)+\Gamma_D^0(|\mathbf{r}-\mathbf{r}'|). \quad (59)$$

From Eq. (54), one obtains the decoherence rate due to the scattering by the condensate:

$$\begin{aligned} \Gamma_D^0(\Delta x_\perp) &= \sum_q (1 - e^{i/\hbar \mathbf{q} \cdot (\mathbf{r} - \mathbf{r}')} ) \Gamma^0(\bar{\mathbf{p}}, \mathbf{q}) \\ &= n_0 \sigma \frac{\bar{p}}{m} \left[ \left( 1 - \frac{\sin(\Delta x_\perp / \lambda_D)}{\Delta x_\perp / \lambda_D} \right) \right. \\ &\quad \left. - 2 \int_{-1}^0 d\cos\theta \frac{\cos\theta}{(1/z) \exp\{\lambda_{dB}^2 / (2\lambda_D)^2 \cos^2\theta\} - 1} \right. \\ &\quad \left. \times \left[ 1 - J_0 \left( 2 \cos\theta \sin\theta \frac{\Delta x_\perp}{\lambda_D} \right) \right] \right]. \quad (60) \end{aligned}$$

The first term of the second line of Eq. (60) gives the decoherence rate due to collisions with the condensate without bosonic enhancement. It resembles the decoherence found for light scattering [12–14], thus referring to the similarities between the two systems. The second term describes the bosonic enhancement of the condensate-induced decoherence. It still involves an integration over the scattering angle  $\theta$  and must be evaluated numerically. The Bose-Einstein distribution included in the integrand favors small values of  $\cos\theta \lambda_{dB} / \lambda_D$ . However, since at  $\cos\theta=0$  the integrand vanishes, the realized scattering angles depend on the ratio  $\lambda_{dB} / \lambda_D$ : A fast beam will result in smaller values of  $\cos\theta$  and therefore in a smaller bosonic enhancement of transverse decoherence than a slow beam. Note that in accordance with the case of a fast beam colliding with a slow Boltzmann gas the decoherence length scale here is set by  $\lambda_D$ .

The decoherence rate due to the beam scattering at the excited phase is given by

$$\begin{aligned} \Gamma_D^\epsilon(\Delta x_\perp) &= \sum_q (1 - e^{i/\hbar \mathbf{q} \cdot (\mathbf{r} - \mathbf{r}')} ) \Gamma^\epsilon(\bar{\mathbf{p}}, \mathbf{q}) \\ &= n_\epsilon \sigma \bar{v} \frac{1}{g_2(z)} \int d\cos\theta \int dk k \\ &\quad \times \frac{(-1)}{1-b} \ln \left[ \frac{1 - z e^{-(k+v)^2}}{1 - z b e^{-(k+v)^2}} \right] \left[ 1 - J_0 \left( k \sin\theta \frac{2}{1+\delta} \frac{\Delta x_\perp}{\lambda_{dB}} \right) \right] \\ &\quad - 2 n_0 \sigma \frac{\bar{p}}{m} \int_{-1}^0 d\cos\theta \frac{[(\delta-1)/(\delta+1)]^2 \cos\theta}{(1/z) \exp\{[(\delta-1)(\delta+1)]^2 \lambda_{dB}^2 / (2\lambda_D)^2 \cos^2\theta\} - 1} \left\{ 1 - J_0 \left[ 2 \cos\theta \sin\theta \left( \frac{\delta-1}{\delta+1} \right)^2 \frac{\Delta x_\perp}{\lambda_D} \right] \right\}. \quad (61) \end{aligned}$$

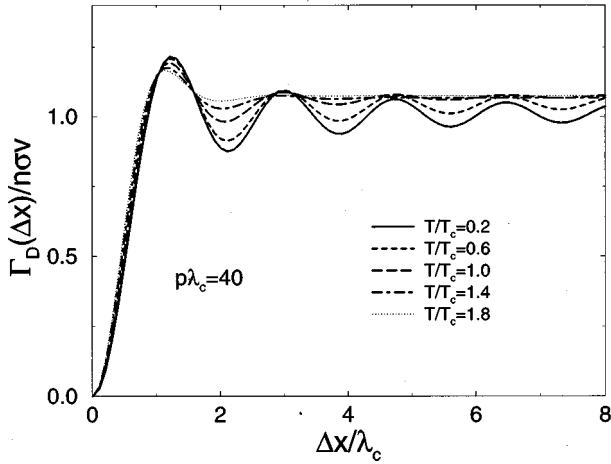


FIG. 4. The decoherence rate  $\Gamma_D(\Delta x)$  due to collisions of a fast atomic beam in a Bose gas versus the width of the coherence  $\Delta x$ . The parameters are  $\rho\lambda_c/\hbar=40$  and  $\delta=0.1$  ( $\lambda_c$  defines the gas's thermal de Broglie wavelength at the critical temperature  $T_c$ ).  $\Gamma_D$  is given in units of the collision rate of the beam at a resting gas,  $n\sigma v = n\sigma p/m$ ,  $\Delta x$  in units of the thermal de Broglie wavelength of the gas at the critical temperature  $T_c$ . The bosonic enhancement of the fast beam's scattering is small because of the large momentum transfer in a collision. The situation resembles Figure 2. In contrast to Figure 2 the oscillations of  $\Gamma_D(\Delta x)$  are less strongly damped.

Here, we used the abbreviations

$$b = e^{\lambda_{dB}^2/\hbar^2 \delta(q^2 + pq\cos\theta)} \quad (62)$$

and

$$n_\epsilon = \frac{N}{V} \left[ \theta(T - T_c) + \left( \frac{T}{T_c} \right)^{3/2} \theta(T_c - T) \right]. \quad (63)$$

$n_\epsilon = (N - N_0)/V$  describes the density of the gas atoms in the excited phase. The integrals in Eq. (61) must be evaluated numerically, taking special care of the integrand's singularity at  $z=1$ . The first term of the second line of Eq. (60) describes the decoherence by the bosonic enhanced fluctuations within the continuous phase, the second term gives the bosonic enhancement of the scattering due to collisions which push a gas atom into the condensate. As we have already observed for the scattering at the condensate, small values of the transferred momentum are favored. Therefore we expect the strongest impact of the bosonic nature of the gas for relatively slow atomic beams.

In Figs. 4 and 5 the decoherence rates are shown for the scattering of an atomic beam from a Bose background gas. In comparison to a Boltzmann gas one could expect a number of new features in the scattering from a Bose gas: On the one hand the bosonic momentum distribution is different, favoring generally smaller gas momenta (especially zero momentum if a condensate exists); on the other hand there is the bosonic enhancement of the scattering due to quantum statistical correlations within the Bose gas. This unique characteristic of the Bose gas is not present in the classical Boltzmann gas.

Figure 4 displays the decoherence rate for a fast atomic beam traversing the gas. The situation turns out to be very similar to that for a Boltzmann gas: The decoherence length

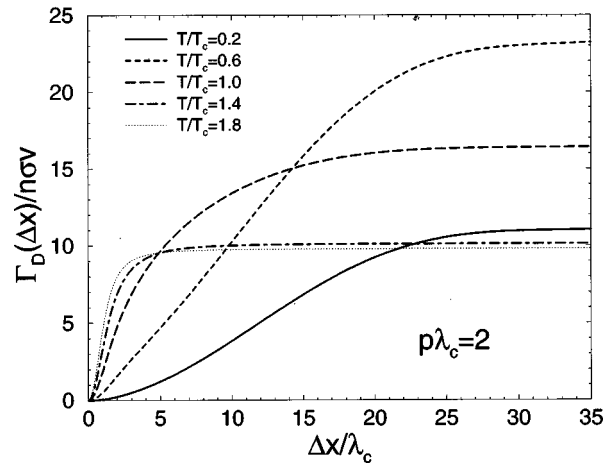


FIG. 5. The decoherence rate  $\Gamma_D(\Delta x)$  due to collisions of a slow atomic beam in a Bose gas. The parameters are  $\rho\lambda_c/\hbar=2$  and  $\delta=0.1$ .  $\Gamma_D$  is given in units of the collision rate at a resting gas,  $\Delta x$  in units of the thermal de Broglie wavelength in the gas at the critical temperature  $T_c$ . Above the critical temperature the length scale of the coherence decay is essentially given by the the gas thermal de Broglie wavelength, the decoherence strength by the slow beam collision rate. In this regime the situation resembles the slow beam scattering in a Boltzmann gas (cf. Fig. 3). However, at and below the critical temperature the decoherence length is widened and the decoherence strength increased due to the strong bosonic enhancement of scatterings with small  $q$ . The bosonic enhancement of the scattering is at first increased, reaches a maximum around  $T=0.6T_c$ , and weakened for lower temperature.

is given by  $\lambda_D$ , the strength is set by the collision rate of the beam. Thus, again, the decoherence rate is governed mainly by beam properties. Nevertheless, the thermal properties of the gas are displayed in the smoothing of the oscillatory behavior of the decoherence rate with increasing temperature. Note that because of the higher coherence of the bosonic gas compared to a Boltzmann gas at the same temperature the oscillations are somewhat stronger in the bosonic case.

However, the scattering of a slow beam at low temperatures shows a remarkable departure from the behavior for the Boltzmann gas: Figure 5 shows the decoherence rate for a number of different gas temperatures. While for temperatures above the critical point the strength and length of the decoherence is similar to the Boltzmann case, we observe for temperatures at and below the critical point two new features. First, the length scale of the decoherence is increasingly stretched the deeper the temperature drops. Comparison with Fig. 3 for the Boltzmann gas (note the different ranges of the abscissa) shows that this is not only due to the increase in the number of very slow atoms but a consequence of the strongly augmented number of collisions with very small momentum transfer  $q$ . Since the dephasing imposed onto the beam is less effective for small  $q$ , this will produce a larger decoherence length.

Second, the rate of collisions (here defined as the plateau value of the decoherence rate for large  $\Delta x$ ) increases with decreasing temperature due to the enhanced scattering until it reaches a maximum at  $T \approx 0.6T_c$ . For lower temperatures the collision rate—and accordingly the decoherence rate—drops again. At  $T=0$  the collision rate corresponds to the classi-

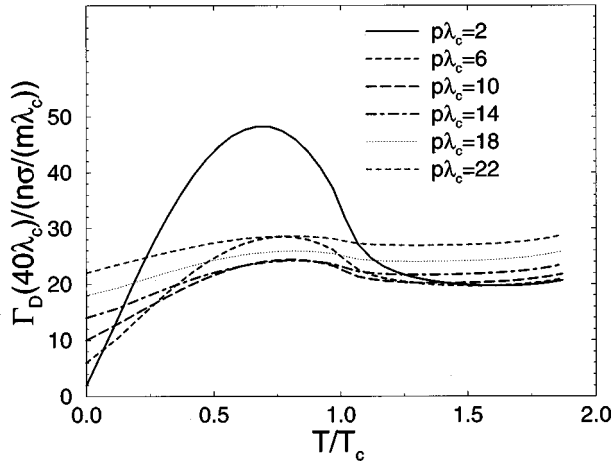


FIG. 6. The rate of collisions of an atomic beam in a Bose gas versus the temperature for different momenta of the beam atom. Here, the rate of collisions is defined as saturation value of the decoherence rate for very wide coherences ( $\Delta x = 40\lambda_c$ ). It is given in units of  $n\sigma/(m\lambda_c)$ . For the slow atomic beam ( $p\lambda_c/\hbar = 2$ ) a strong bosonic enhancement of scattering is visible even before the critical point is reached. Its maximum lies around  $T = 0.6T_c$ . For larger beam momenta the bosonic enhancement of scattering is only weak. At very low temperatures the rate of collisions is reduced to  $n\sigma v$ , as is to be expected classically. The quantum statistical enhancement of the scattering does not play a major role here, since the number of atoms that could be accommodated in the continuous phase space and along with it the number of final states for the gas atom after the scattering is steadily reduced.

cally expected result  $\Gamma_c = n\sigma v$  for the scattering of the beam at a collection of gas atoms at rest.

Figure 6 displays the dependence of the collision rate on the temperature for a number of different beam momenta. While for a fast atomic beam the bosonic enhancement of the scattering is barely visible, we find for the slow beam a strong increase in the scattering due to the bosonic enhancement of the scattering. The enhancement factor  $[1 + n_{\text{BE}}(\mathbf{p}_G - \mathbf{q})]$  results in an additional scattering contribution proportional to  $n_{\text{BE}}(\mathbf{p}_G)n_{\text{BE}}(\mathbf{p}_G - \mathbf{q})$  due to the bosonic enhancement. However, this bosonic enhancement does not prevail all down to zero temperature: The additional bosonic contribution due to  $n_{\text{BE}}(\mathbf{p}_G)n_{\text{BE}}(\mathbf{p}_G - \mathbf{q})$  depends on the availability of phase space for the gas atom not only before the scattering  $[n_{\text{BE}}(\mathbf{p}_G)]$  but also after the scattering ( $n_{\text{BE}}(\mathbf{p}_G - \mathbf{q})$ ). Because the amount of available phase space at  $|\mathbf{p}_G| > 0$  shrinks down to zero at  $T = 0$ ,  $n_{\text{BE}}(\mathbf{p}_G)$  vanishes for  $|\mathbf{p}_G| > 0$  and so does any bosonic enhancement proportional to  $n_{\text{BE}}(\mathbf{p}_G)n_{\text{BE}}(\mathbf{p}_G - \mathbf{q})$ . Thus the quantum statistical enhancement of the scattering will find a maximum value at some temperature between zero and  $T_c$  where phase space at  $|\mathbf{p}_G| > 0$  as well as phase space at  $\mathbf{p}_G = \mathbf{0}$  in the condensate is available.

### C. Effects of decoherence

In the absence of an external potential the solution of the master equations (50), respectively, Eq. (53), is given by

$$\begin{aligned} \rho(\mathbf{r}, \mathbf{r}', t) = & \sum_{p, p', \bar{r}, \bar{r}'} e^{(i/\hbar)\mathbf{p} \cdot (\mathbf{r} - \bar{\mathbf{r}})} e^{-(i/\hbar)(p^2/2m)t} \\ & \times e^{-\Gamma_D(|\bar{\mathbf{r}} - \bar{\mathbf{r}}'|)t} \rho(\bar{\mathbf{r}}, \bar{\mathbf{r}}'; 0) \\ & \times e^{(i/\hbar)(p'^2/2m)t} e^{-(i/\hbar)\mathbf{p}' \cdot (\mathbf{r}' - \bar{\mathbf{r}}')}, \end{aligned} \quad (64)$$

where  $\rho(\bar{\mathbf{r}}, \bar{\mathbf{r}}'; 0)$  is the initial density operator of the beam. The consequences of the loss of coherence after the beam's passage through a background gas in an atomic interferometer can be read off from the interference pattern produced by the beam. The intensity on the screen is proportional to the probability  $\rho(\mathbf{r}_0, \mathbf{r}_0; t)$  of finding a single beam atom at position  $\mathbf{r}_0$  and time  $t$  on the screen. The initial condition,  $\rho(\bar{\mathbf{r}}, \bar{\mathbf{r}}'; 0)$ , is given by the beam atom's density matrix at the entry of the interferometer at time  $t = 0$ .

If there are no collisions the evolution is entirely coherent [ $\Gamma_D(|\bar{\mathbf{r}} - \bar{\mathbf{r}}'|) = 0$ ]. In this case the probability  $P_0(\mathbf{r}_0, t)$  to find a beam atom at position  $\mathbf{r}_0$  in the interference pattern on the screen is

$$\begin{aligned} P_0(\mathbf{r}_0) = & \sum_{p, p', \bar{r}, \bar{r}'} e^{(i/\hbar)\mathbf{p} \cdot (\mathbf{r}_0 - \bar{\mathbf{r}})} e^{-(i/\hbar)(p^2/2m)t} \\ & \times \rho(\bar{\mathbf{r}}, \bar{\mathbf{r}}'; 0) e^{(i/\hbar)(p'^2/2m)t} e^{-(i/\hbar)\mathbf{p}' \cdot (\mathbf{r}_0 - \bar{\mathbf{r}}')}. \end{aligned} \quad (65)$$

In the case of an incoherent evolution in the presence of collisions, we can calculate from Eq. (64) the probability  $P_{\text{coll}}$  of finding a beam atom at position  $\mathbf{r}_0$  on the screen:

$$\begin{aligned} P_{\text{coll}}(\mathbf{r}_0, t) = & \sum_{\bar{r}, \bar{r}'} e^{-\Gamma_D(|\bar{\mathbf{r}} - \bar{\mathbf{r}}'|)t} \sum_{p, p'} e^{(i/\hbar)\mathbf{p} \cdot (\mathbf{r}_0 - \bar{\mathbf{r}})} \\ & \times e^{-(i/\hbar)(p^2/2m)t} \rho(\bar{\mathbf{r}}, \bar{\mathbf{r}}'; 0) \\ & \times e^{(i/\hbar)(p'^2/2m)t} e^{-(i/\hbar)\mathbf{p}' \cdot (\mathbf{r}_0 - \bar{\mathbf{r}}')}. \end{aligned} \quad (66)$$

By inserting

$$1 = \int d^3\Delta \int d^2\mathbf{k} e^{-i\mathbf{k} \cdot (\mathbf{r} - \mathbf{r}' - \Delta)} \quad (67)$$

we obtain

$$\begin{aligned} P_{\text{coll}} = & \int d^3\Delta e^{-\Gamma_D(|\Delta|)t} \sum_{\bar{r}, \bar{r}'} \frac{1}{(2\pi)^3} \\ & \times \int d^3\mathbf{k} e^{i\mathbf{k} \cdot [\Delta - (\bar{\mathbf{r}} - \bar{\mathbf{r}}')]} \\ & \times \sum_{p, p'} e^{(i/\hbar)\mathbf{p} \cdot (\mathbf{r}_0 - \bar{\mathbf{r}})} e^{-(i/\hbar)(p^2/2m)t} \rho(\bar{\mathbf{r}}, \bar{\mathbf{r}}'; 0) \\ & \times e^{(i/\hbar)(p'^2/2m)t} e^{-(i/\hbar)\mathbf{p}' \cdot (\mathbf{r}_0 - \bar{\mathbf{r}}')}. \end{aligned} \quad (68)$$

Using the definition of  $P_0$  (the probability without background gas), the probability of finding a beam atom at position  $\mathbf{r}_0$  in the presence of collisions can be expressed as

$$P_{\text{coll}}(\mathbf{r}_0, t) = \frac{1}{(2\pi)^3} \int d^3\mathbf{k} G(\mathbf{k}) P_0(\mathbf{r}_0 + \hbar\mathbf{k}t/m, t), \quad (69)$$

where we have defined

$$G(\mathbf{k}) = \int d^3\Delta e^{i\Delta \cdot \mathbf{k}} e^{-\Gamma_D(|\Delta|)t}. \quad (70)$$

Hence the position density in the presence of collisions,  $P_{\text{coll}}(\mathbf{r}_0, t)$ , is the convolution of the coherent position distribution  $P_0(\mathbf{r}_0, t)$ , in the absence of collisions, with a collision kernel  $G(\mathbf{k})$ . The momenta  $\hbar\mathbf{k}$  here do not refer to single collisions, but correspond to the sum of recoils experienced by the atom in the course of the interaction. Thus the coherent position distribution  $P_0(\mathbf{r}_0, t)$  is smeared out due to the collisions with the background gas. The smearing factor is given by the Fourier transform of the decoherence rate  $\Gamma_D(|\Delta|)$ .

#### D. Visibility

We will now investigate the influence of decoherence on the interference pattern behind a double slit in greater detail. The coherent probability distribution is given by the modulus square of the beam wave function  $\psi(\mathbf{r}_0, t)$  on the screen,

$$P_0(\mathbf{r}_0, t) = |\psi(\mathbf{r}_0, t)|^2, \quad (71)$$

where

$$\psi(\mathbf{r}_0, t) = \sum_{\mathbf{p}} e^{(i/\hbar)\mathbf{r}_0 \cdot \mathbf{p} - (i/\hbar)(p^2/2m)t} \sum_{\mathbf{r}} e^{-i/\hbar \mathbf{p} \cdot \mathbf{r}} \psi(\mathbf{r}, 0). \quad (72)$$

The initial wave function  $\psi(\mathbf{r}, 0)$  describes the beam atom within the double slit:

$$\psi(\mathbf{r}, 0) = \frac{1}{\sqrt{2}} [s(x - x_L) + s(x - x_R)] \phi_{\parallel}(y, z). \quad (73)$$

Here,  $s(x)$  gives the wave function's profile within one of the slits.  $\phi_{\parallel}(y, z)$  describes the longitudinal degrees of freedom of the beam, which will be neglected in the following. In a first approximation to an experimentally realistic transmission profile we take  $s(x)$  to be a Gaussian of width  $a$ . After integrating Eq. (72) and replacing the time of flight  $t$  of the beam over the distance  $l$  to the screen by  $t = lm/\bar{p}$ , we obtain for the wave function on the screen

$$\begin{aligned} \psi(x_0) \propto & e^{i[x_0 - x_L]^2/2l} (\bar{p}/\hbar) e^{-[(x_0 - x_L)^2/l^2]/(a^2\bar{p}^2/4\hbar^2)} \\ & + e^{i[x_0 - x_R]^2/2l} (\bar{p}/\hbar) e^{-[(x_0 - x_R)^2/l^2]/(a^2\bar{p}^2/4\hbar^2)}. \end{aligned} \quad (74)$$

If the screen is in the far field of the diffraction ( $x_0 \gg x_L, x_R$ ) we can approximate the diffraction angle by

$$\frac{x_0 - x_L}{l} \approx \tan\alpha \approx \frac{x_0 - x_R}{l} \quad (75)$$

and obtain

$$\begin{aligned} \psi(x_0) \propto & e^{-\tan^2\alpha a^2 \bar{p}^2/4\hbar^2} e^{i(1/2)\tan\alpha x_0(\bar{p}/\hbar)} (e^{i(1/2)\tan\alpha x_L(\bar{p}/\hbar)} \\ & + e^{i(1/2)\tan\alpha x_R(\bar{p}/\hbar)}). \end{aligned} \quad (76)$$

This yields

$$P_0(x_0) \propto e^{-\tan^2\alpha a^2 \bar{p}^2/2\hbar^2} \left[ 1 + \cos\left(\frac{1}{2}\tan\alpha \frac{\bar{p}}{\hbar} (x_L - x_R)\right) \right]. \quad (77)$$

In the limit of a wide slit separation ( $a \ll |x_R - x_L|$ ) we can neglect the modification of the central interference pattern by the diffraction at the single slits. This yields for the diffraction pattern

$$P_0(x_0) \propto 1 + \cos\left(\frac{1}{2}\tan\alpha \frac{\bar{p}}{\hbar} (x_L - x_R)\right). \quad (78)$$

The position distribution  $P_0(x_0)$  is directly proportional to the diffraction pattern on the screen.

The resolution of the pattern can be characterized by the visibility  $\mathcal{V}$ :

$$\mathcal{V} = \frac{P_0^{\max} - P_0^{\min}}{P_0^{\max} + P_0^{\min}}. \quad (79)$$

From Eq. (77) we calculate the visibility of the coherent diffraction pattern (without collisions) as

$$\mathcal{V}_{\text{coh}} = 1. \quad (80)$$

Relation (69) allows us to obtain the incoherent diffraction pattern easily in terms of  $P_0$ :

$$P_{\text{coll}}(x_0) \propto 1 + e^{-\Gamma_D(x_L - x_R)(lm/\bar{p})} \cos\left(\frac{1}{2}\tan\alpha \frac{\bar{p}}{\hbar} (x_L - x_R)\right). \quad (81)$$

Because of the collision-induced decoherence effect, the visibility is reduced to

$$\mathcal{V}_{\text{coll}} = e^{-\Gamma_D(x_L - x_R)(lm/\bar{p})}. \quad (82)$$

The visibility of the incoherent diffraction pattern renders a direct image of the decay of the beam's coherence behind the slits. The result (82) in principle holds for a grid as well, since the visibility behind a grid is essentially determined by the interference between neighboring slits.

Figures 7 and 8 show the visibility of the interference pattern produced by a slow (fast) atomic beam traversing a Boltzmann gas as a function of the gas temperature for a number of different slit separations. Since for a slow beam the decoherence length is essentially given by the gas's thermal de Broglie wavelength, a decrease in temperature results in a longer decoherence length and thus in a higher visibility in Fig. 7. However, in Fig. 8 the temperature dependence is mainly due to the smoothing of the oscillations in the decoherence rate (cf. Fig. 2). This leads to an "anomalous" behavior of the visibility, producing lower visibility with lower temperature.

In Figs. 9 and 10 the visibility of the interference pattern after traversing a Bose gas are presented. Figure 9 treats the

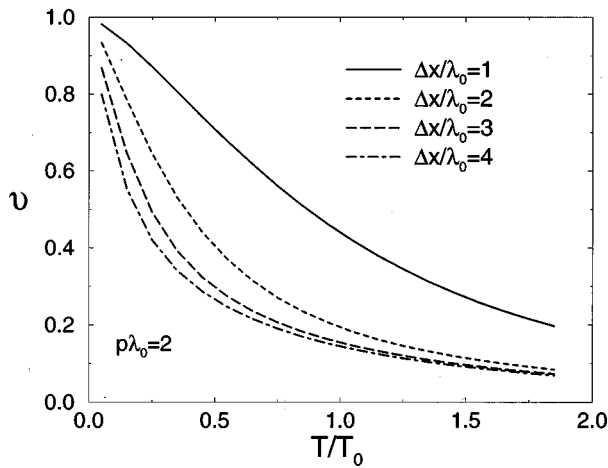


FIG. 7. The visibility  $\mathcal{V}$  versus the temperature  $T$  for a slow, heavy beam traversing a Boltzmann gas ( $p\lambda_0/\hbar=2, \delta=0.1$ ). Here, the time of flight through the gas is  $\tau=\Gamma_c(T_0)^{-1}$ , i.e., at temperature  $T_0$  there is approximately one collision between the double slit and the screen. Enlarging the width of the coherence  $\Delta x$  leads to a stronger decay of the visibility with temperature.

case of a relatively narrow slit separation: Here, the situation is qualitatively similar to the results for a Boltzmann gas. The lower the temperature, the higher the visibility. Although for slow beams the quantum statistical enhancement of the scattering is considerable, it does not contribute essentially to the decoherence of the beam, since for a narrow coherence the enhancement in scattering is compensated by a stretching of the decoherence length, so that the decoherence rate does not depart considerably from the situation encoun-

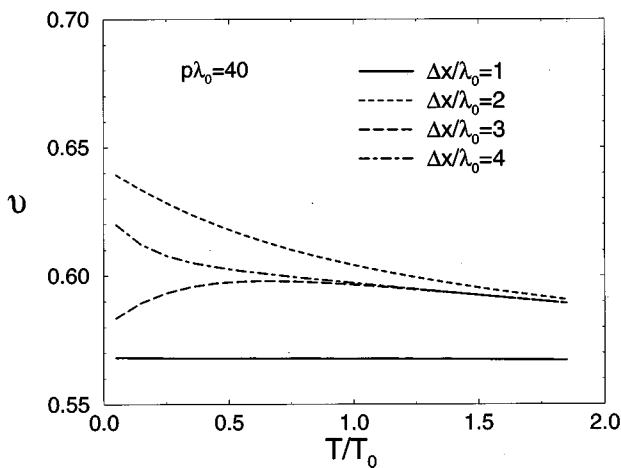


FIG. 8. The visibility  $\mathcal{V}$  versus the temperature  $T$  for a fast, heavy beam traversing a Boltzmann gas ( $p\lambda_0/\hbar=40, \delta=0.1$ ). Here, the time of flight through the gas is  $\tau=0.25(n\sigma v)^{-1}$ , i.e., there are approximately 0.25 collisions between the double slit and the screen. Since at  $\Delta x=\lambda_0$  the decoherence rate is maximum (almost independent of temperature) the visibility for this curve does not vary appreciably with temperature. For  $\Delta x=2\lambda_0$  the visibility shows an anomalous temperature dependence: In spite of a decrease in temperature the visibility worsens. This relates to the damping of the oscillations in the decoherence rate with increasing temperature, which leads to an increase of decoherence for dropping temperatures at  $\Delta x=2\lambda_0$ .

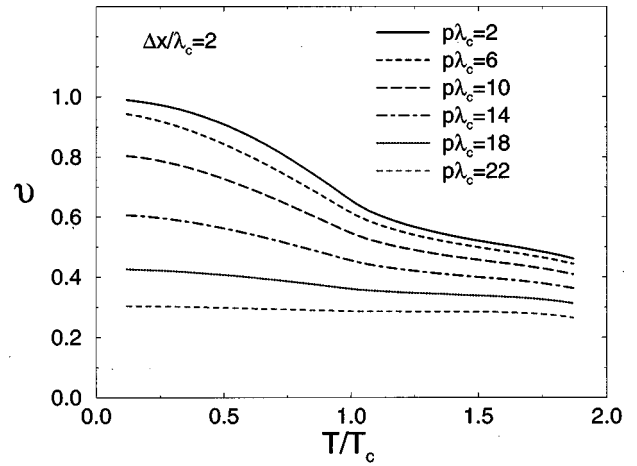


FIG. 9. The visibility  $\mathcal{V}$  versus the temperature  $T$  for  $\Delta x=2\lambda_c$ . The curve is plotted for six different beam momenta. The time of flight through the gas is given such that the fastest beam ( $p\lambda_c/\hbar=22$ ) experiences on average one collision. Since for slow beams below the critical point the decoherence length scale is extended the visibility is improved in this regime. However, for fast beams, due to the only weak temperature dependence of the decoherence the improvement of the visibility is small.

tered in a Boltzmann gas. Nevertheless, for a wide slit separation the quantum statistically enhanced scattering has its full impact on the visibility: Figure 10 displays the visibility versus temperature for a number of different beam velocities. As already pointed out, around the critical point the decoherence and therefore also the loss in visibility are strongly increasing because of the wide coherence of a slow beam. At fixed volume and particle number, the visibility reaches a minimum at around  $t=0.6T_c$ . For even lower temperatures the visibility increases again, according to the diminished

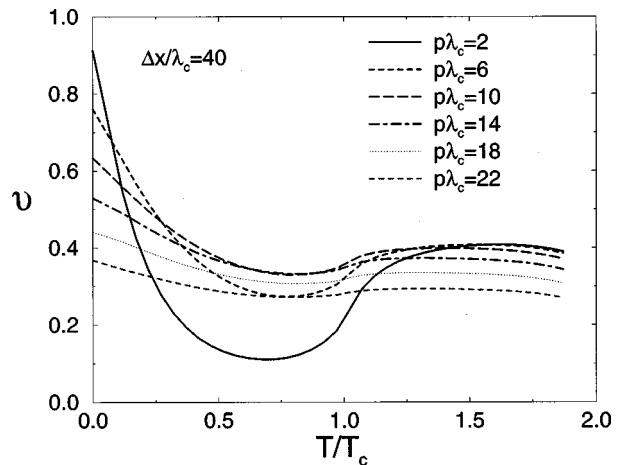


FIG. 10. The visibility  $\mathcal{V}$  versus the temperature for  $\Delta x=40\lambda_c$ . The curve is plotted for six different beam momenta. The time of flight through the gas is given by  $\tau=n\sigma\hbar/(m\lambda_c)$ . For small momenta there is a marked reduction of the visibility due to the bosonic enhancement of scattering around the critical temperature. However, for very low temperatures the excited phase begins to be depleted, so the bosonic enhanced scattering is reduced, leading to a recovery of the visibility. At  $T=0$  this results in the expected classical picture of beam collision with a resting gas.

scattering. The loss of beam coherence around the critical point as observed in the diffraction pattern is entirely due to the quantum fluctuations of the Bose gas around the critical point. Thus we see here the signature of Bose-Einstein condensation taking place.

#### IV. CONCLUSION

In this paper we have studied how atom interferometry may be used to investigate the coherence properties of a dilute gas traversed by an atomic beam. Special attention was paid to a condensing Bose gas. Since the visibility of the interference pattern depends on the coherence of the beam, one can infer the decoherence suffered by the beam from the loss of visibility. In turn the decoherence may be used as a probe for the coherence properties of the traversed medium interacting with the beam. Thus the strong forward scattering of a heavy beam in connection with the small probability of multiple scattering constitutes an effective probe for investigating a gas. To study the probing theoretically we derived a master equation for the beam atom, restricting ourselves to two-body collisions and  $s$ -wave approximation. Special care was taken to derive a Lindblad form of the master equation thereby ensuring the positivity of the beam's density operator in the course of the interaction. We have found that one should distinguish between two qualitatively different situations: An atomic beam that is either fast compared to the gas velocities or slow. In the first situation, the decoherence length is essentially determined by the de Broglie wavelength of the atomic beam itself, scaled by a factor accounting for the ratio between gas and beam masses. The strength of the decoherence is set by the classical rate of collisions between the beam atom and the almost resting gas atoms. The second situation, namely, the slow beam, enables an observation of the gas properties in the beam decoherence: The decoherence length is set by the gas thermal de Broglie wavelength, the decoherence strength is given by the rate of

collisions between gas and atoms. If we study the scattering in a condensing Bose gas we encounter a quantum statistical enhancement of the scattering, especially for small momentum transfer. Whereas the smallness of the momentum transfer for narrow beam coherences compensates the enhanced scattering, thereby masking the quantum correlations in the gas as observed in the interference pattern, one can see the full impact of the quantum statistically enhanced decoherence in the marked decrease of visibility around the critical point. Although we have treated here the decoherence of an atomic beam in an ideal and free gas the results here point to the possibility of observing the signature of Bose-Einstein condensation in trapped gas via atomic interferometry. However, very close to temperature  $T=0$  weak interatomic interactions will spoil the picture given by an ideal gas: Diagonalization of the weak interaction, e.g., by a Bogoliubov transformation, will lead to a linear quasiparticle dispersion relation for small energies. Since the excitation of a quasiparticle from the quasiparticle vacuum to a quasiparticle state on the linear branch of the dispersion relation by a collision with a beam atom is forbidden due to energy and momentum conservation a gas at  $T=0$  will not transfer momentum to the beam, the gas thus being transparent to the beam. This effect analogous to superfluidity will prevent decoherence and therefore lead to perfect visibility at  $T=0$ . This means that via atom interferometry it is not only possible to observe the onset of Bose-Einstein condensation thanks to quantum statistically enhanced scattering but also the transition to a regime in the vicinity of  $T=0$  where the weak interactions within the gas become dominant compared to the near ideal behavior of the gas at higher temperatures.

#### ACKNOWLEDGMENT

The authors appreciate valuable discussions with M. Naraschewski.

- 
- [1] M. H. Anderson *et al.*, *Science* **269**, 198 (1995).
  - [2] C. C. Bradley, C. A. Sackett, J. J. Tollet, and R. G. Hulet, *Phys. Rev. Lett.* **75**, 1687 (1995).
  - [3] K. B. Davis *et al.*, *Phys. Rev. Lett.* **75**, 3969 (1995).
  - [4] M. R. Andrews *et al.*, *Science* **273**, 84 (1996).
  - [5] W. H. Zurek, *Phys. Today* **44(10)**, 36 (1991).
  - [6] C. W. Gardiner, *Quantum Noise* (Springer-Verlag, Berlin, 1991).
  - [7] C. Cohen-Tannoudji, in *Frontiers in Laser Spectroscopy*, edited by S. Haroche and S. Liberman (North-Holland, Amsterdam, 1977), p. 4.
  - [8] L. Diósi, *Europhys. Lett.* **30**, 63 (1995).
  - [9] K. Huang, *Statistical Mechanics* (John Wiley & Sons, New York, 1987).
  - [10] C. Cohen-Tannoudji, B. Diu, and Franck Laloë, *Quantum Mechanics* (John Wiley & Sons, New York, 1977), Vol. II.
  - [11] A. L. Fetter and J. D. Walecka, *Quantum Theory of Many-Particle Systems* (McGraw-Hill, New York, 1971).
  - [12] S. M. Tan and D. F. Walls, *Phys. Rev. A* **47**, 4663 (1993).
  - [13] T. P. Altenmüller and A. Schenzle, *Phys. Rev. A* **49**, 2016 (1994).
  - [14] O. Steuernagel and H. Paul, *Phys. Rev. A* **52**, R905 (1995).